IL NUOVO CIMENTO **45 C** (2022) 198
DOI 10.1393/ncc/i2022-22198-0

COMMUNICATIONS: SIF Congress 2021

Cryogenic vacuum behavior of porous materials of interest for future accelerators

M. ANGELUCCI(*)

INFN, Laboratori Nazionali di Frascati - 00044 Frascati, Italy

received 31 January 2022

Summary. — The properties of vacuum components at cryogenic temperature represent a crucial aspect to assure accelerator's best performances. These are not only intrinsic to each surface, but also to the residual gas physisorbed on the walls and to the many interactions such surfaces will undergo during operation. Here we report a study on the effects induced by temperature fluctuations and electron irradiation on a class of porous materials which are potential candidates for future accelerators. The results will be useful to predict the gas quantity delivered in cryogenic vacuum from porous surfaces.

1. – Introduction

The operation and performance of modern high-energy charged particle accelerators are strongly affected by low-energy electron generated in vacuum chamber by photoemission, residual-gas ionization and secondary emission. These electrons can induce increases in vacuum pressure, emittance growth, beam instabilities, beam losses, beam lifetime reductions, or additional heat loads on cold chamber walls [1-5]. Moreover, interacting with the positive beam, the electrons will be accelerated gaining energy and finally will hit the vacuum chamber walls. There, they will generate additional secondary electrons, whose number is governed by the secondary electron yield (SEY) of the wall surface. If SEY (*i.e.*, the number of secondary electrons generated per incident one) is larger than unity, the electron population will multiply with successive bunch passages. This can lead to the formation of an increasingly high density of electrons and to the so-called electron-cloud effects (ECEs). One powerful method to control and overcome such effects is to construct accelerators vacuum chambers with a low SEY surface, ideally always less than or just around one. An efficient ECEs mitigation strategy is nowadays considered as a top priority challenge for the commissioning of the High-Luminosity Large Hadron

(*) E-mail: marco.angelucci@lnf.infn.it

Collider (HL-LHC) [6] and for the proton-proton Future Circular Collider (FCC-hh) [7] Surface geometrical modification has been proved to be quite effective to this purpose. In particular, a porous morphology formed by different scale structures, micro- and sub-micrometrical grooves can be reached by treating a metallic substrate by laser ablation surface engineering (LASE). This method is extremely successful in reducing SEY below 1 [8-11]. However, the sub-micrometric structure significantly increases the effective surface available in the porous materials compared with that of their flat counterpart. If, on one hand, this results in re-adsorption of secondary electrons in the structure giving a low SEY, on the other hand this could certainly influence their vacuum behavior. Moreover, a yet more severe issue arises when considering using such LASE treated surfaces at cryogenic temperatures (T). If T is low enough, residual gas molecules such as H_2, CO, CO_2, H_2O, and CH_4 may be adsorbed on the cryogenic walls.

During the accelerator's operation, vacuum is influenced by the gas desorption induced by temperature fluctuation and by the interaction of electron, photon and ion with the vacuum chamber wall. The desorption of these molecules may induce an unwanted pressure increase [12] that may indeed have significant detrimental effects on machine performances. For this reason, it is essential to investigate these systems through Thermal Programmed Desorption (TPD) and Electron Stimulated Desorption (ESD). These studies can give a correct evaluation of the allowed temperature fluctuation range and the relative amount of gas finally delivered inside the vacuum chambers. Here, the vacuum behavior of a flat and a porous (LASE) surface is presented and analyzed following gas desorption as a function of temperature and electrons irradiation.

2. – Experimental details

Experiments were performed in an ultra high vacuum (UHV) μ-metal chamber at the "Material Science" laboratory of the INF-LNF (Frascati, Italy). The setup has been described elsewhere [1, 3, 13, 14]. Two categories of 8×8 mm^2 Cu samples were investigated: a sputtered clean "flat" Cu substrate consisting of Oxygen-Free High Conductivity (OFHC), and a representative sample from the LASE-Cu material family. It is an OFHC copper sheet of some hundreds of microns, colaminated on stainless steel and then laser treated by R. Valizadeh *et al.* at the Science & Technology Facility Council (STFC) [8]. The dosing units are given in Langumir ($1\,\mathrm{L} = 1.33 \times 10^{-6}\,\mathrm{mbar\ s}$). Desorptions are measured by using a quadrupole mass spectrometer (QMS, Hiden, HAL 3F PIC). TPD investigations are performed by heating the sample with a rate of 0.005 K/s. TPD curves are given in molecules (or atoms, in the case of Ar) per unit of geometrical area, which is independent from surface morphology. To evaluate Electron Stimulated Desorption yield (η, the number of desorbed atoms per incident electron), the sample is irradiated by an electron beam of the order of 1 mm^2, emitted by a Kimball Physics electron gun equipped with a standard Tungsten cathode. The sample temperature is hold at 10 K in order to prevent thermal outgassing during measurements.

3. – Results and discussion

In fig. 1, the desorption results for 10, 25 and 100 L Ar and 10, 25 and 50 L of CH_4 dosed on flat Cu and LASE-Cu are reported. When measuring TPD from the flat surface, a sharp peak is observed for both species. This sharp single peak corresponds to the desorption of a condensed thick layer of the specific gas and its temperature is determined by the weak Van der Waals interaction energies between molecules [15].

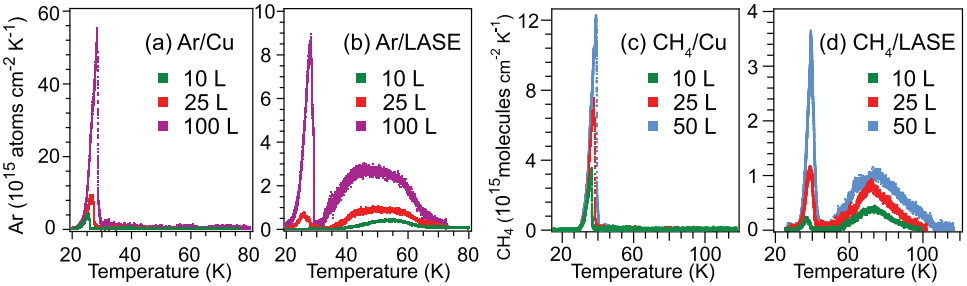

Fig. 1. – TPD curves of different Ar and CH_4 doses on flat Cu and LASE-Cu [13, 14].

In agreement with the literature, the desorption temperature can be estimated around 28–30 K for Ar and around 35–39 K for CH_4. The desorption of Ar atoms and CH_4 molecules from the LASE sample can be divided into two parts: i) a sharp peak in the same temperature range and with the same nature as that observed from the flat surface, ii) a broad peak between 35 and 70 K for Ar and between 40 and 100 K for CH_4. Laser treatment not only increases the area accessible to atomic/molecular species but also, its nanostructured morphology determines a local increase of the adsorption energy for atoms/molecules in correspondence of undercoordinated sites and defects [16]. For this reason, the desorption of atoms/molecules close to defected surfaces and/or trapped in the pores of the LASE-Cu surface is shifted to higher temperatures.

Figure 2 shows the comparison between η for different Ar doses on flat and porous substrates. η increases with Ar dose for both surfaces. η from the LASE-Cu is lower then η from the flat Cu for all gas doses. These data are in agreement with those reported in the literature [17].

All these results can be explained considering two main effects of the morphological features. First, since the porous material has a high specific surface with respect to its flat counterpart, the same gas dosing determines a different coverage on the two different substrates. This explains the differences in the total amount gas desorption in TPD and ESD form flat and LASE surfaces. The porous nature of LASE-Cu sample acts like a "trap". This is reflected by a higher number of molecules (or atoms) adsorbed and, then, desorbed for thermal activation. On the other hand, since the transport of secondary electrons is the main mechanism governing ESD [18], a dependence of η on SEY is expected. Considering the lower SEY, this could explain the lower electron

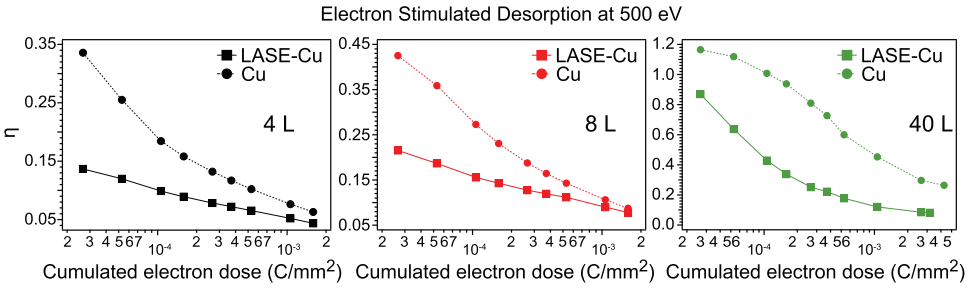

Fig. 2. – η for flat Cu and LASE-Cu at different Ar coverages.

stimulated desorption from the LASE-Cu with respect to the flat sample. This interesting evidence needs further investigation. These results have also to be extended to other gases representative for the real vacuum composition in accelerators.

4. – Conclusions

In this paper, we investigated the role of the morphological modifications in determining the vacuum behavior of a class of porous materials at cryogenic temperatures under thermal variation and electron irradiation. The TPD curves show a vaster and higher desorption temperature range with respect to the one observed from the flat substrates. On the other hand, a lower desorption yield is observed under electron irradiation. Both these results give useful information for using porous surfaces as ECEs mitigators at cryogenic temperatures. While the use and optimization of LASE to mitigate ECEs is quite advanced, a significant additional experimental campaign is necessary to validate their use in future accelerators. In fact, all the dynamic processes that always occur during accelerator's operation (such as thermal, ions, electrons, and photons stimulated desorption) need to be carefully taken into account in order to confirm the compliance with the usually very stringent vacuum requirements of most cryogenic accelerators.

* * *

This work was supported by the ARYA project funded by INFN Scientific National Committee 5. The author thanks R. Cimino, L. Spallino and R. Larciprete for stimulating discussions; V. Baglin, P. Chiggiato, R. Kersevan, O. Malyshev, and R. Valizadeh for useful discussions and for the LASE samples. The author acknowledges the DAΦNE-L team for technical assistance.

REFERENCES

[1] Cimino R. and Demma T., *Int. J. Mod. Phys. A*, **29** (2014) 1430023.
[2] Rumolo G. *et al.*, *Phys. Rev. ST Accel. Beams*, **6** (2003) 081002.
[3] Cimino R. *et al.*, *Phys. Rev. Lett.*, **93** (2004) 014801.
[4] Zimmermann F., *Phys. Rev. ST Accel. Beams*, **7** (2004) 124801.
[5] Ohmi K. *et al.*, *CERN Technical Report*, No. CERN-ACC-2015-285 (CERN, Geneva, Switzerland) 2015.
[6] Apollinari G. *et al.*, *High-Luminosity Large Hadron Collider (HL-LHC): Technical Design Report* (CERN) 2017.
[7] See `http://fcc.web.cern.ch/` for details on the project.
[8] Valizadeh R. *et al.*, *Appl. Phys. Lett.*, **105** (2014) 231605.
[9] Pivi M. *et al.*, *J. Appl. Phys.*, **104** (2008) 104904.
[10] Krasnov A., *Vacuum*, **73** (2004) 195.
[11] Nistor V. *et al.*, *Appl. Surf. Sci.*, **315** (2014) 445.
[12] Benvenuti C. *et al.*, *Vacuum*, **53** (1999) 219.
[13] Spallino L. *et al.*, *Appl. Phys. Lett.*, **114** (2019) 153103.
[14] Spallino L. *et al.*, *Phys. Rev. Accel. Beams*, **23** (2020) 063201.
[15] Honig R. E. and Hook H. O., *RCA Rev.*, **21** (1960) 360.
[16] Park J.-Y. *et al.*, *Phys. Rev. B*, **60** (1999) 16934.
[17] Hannah A. N. *et al.*, *Vacuum*, **189** (2021) 110210.
[18] Dupuy R. *et al.*, *J. Appl. Phys.*, **128** (2020) 175304.